

A POSSIBLE EVIDENCE OF THE GLUON CONDENSATION EFFECT IN COSMIC POSITRON AND GAMMA-RAY SPECTRA

WEI ZHU^{1*}, PENG LIU¹, JIANHONG RUAN¹ AND FAN WANG²

¹Department of Physics, East China Normal University, Shanghai 200241, China

²Department of Physics, Nanjing University, Nanjing, 210093, China

Draft version January 1, 2020

ABSTRACT

The gluon condensation effect in cosmic proton-proton collisions at high energy is used to explain an excess in the positron spectrum observed by AMS. We find that this excess may originate from the GC-effect in Tycho's supernova remnant.

Subject headings: Gluon condensation; Broken power-law; Gamma ray spectrum; Positron spectrum

1. INTRODUCTION

The precise measurement of the positron flux in cosmic rays (CRs) with the Alpha Magnetic Spectrometer (AMS) on the International Space Station exhibits complex energy dependence (Aguilar et al.2019). The results show that a significant excess is added on a diffuse background around 300 ~ 400 GeV of the positron energy. A new extra source is predominantly suggested as dark matter annihilation or other astrophysical sources. A following key point is where is this local source? We can't "see" dark matter. We also can't track the positron because of their complex trajectories in interstellar space. While if we know this extra source radiates a characteristic gamma-ray spectrum, which is closely related to the excessive positrons, then we can find the extra source. The GC mechanism provides this possibility.

Gluons inside proton dominate the proton collisions at high energy and their distributions obey the evolution equations based on Quantum Chromodynamics (QCD). QCD analysis shows that the evolution equations will become nonlinear due to the initial gluons correlations at high energy and these will result in the chaotic solution beginning at a threshold energy (Zhu et al, 2008; Zhu et al, 2006). Most surprisingly, the dramatic chaotic oscillations produce strong shadowing and antishadowing effects, they converge gluons to a state at a critical momentum (Zhu et al, 2017). This is the gluon condensation (GC) in proton. The GC should induce significant effects in the proton collision processes, provided the collision energy is higher than the GC-threshold E_{p-p}^{GC} . The GC model was used to explain the excess in the fluxes of cosmic gamma-ray and electron-positron (Feng et al. 2018; Zhu et al. 2018).

In this work we will present a new evidence, which shows that the positron excess observed by AMS originates from the GC-effect in Tycho's supernova remnant. Our idea is straightforward. High energy gamma-ray and electron-positron fluxes in CRs may originate from leptonic processes (bremsstrahlung, inverse Compton scattering and electromagnetic acceleration mechanism), they are also the products in hadronic processes, where $p + p \rightarrow \pi^0 \rightarrow 2\gamma$, and through strong electromagnetic field inside source $\gamma \rightarrow e^+ + e^-$. We take hadronic

framework but add the GC-effect in this work. When a large amount of gluons condense in a critical momentum space, it must inevitably increase the number of secondary particles (π, γ, e^+ and e^-) at the corresponding energy threshold and breaks the power-law. In particular, the positron excess always accompanied by a special broken gamma-ray spectrum since a considerable part of these two fluxes (see Equations (2.10) and (2.13)) are interrelated. It implies that the gamma-ray spectrum corresponding to the excess positron flux has its characteristic shape. Thus, we can judge which source produces the AMS positron excess using a directly observable gamma-ray spectrum.

We will give the relating formulas of the GC model for the explanation of gamma-ray and positron flux in Section 2. A detailed description can be found in (Feng et al.2018; Zhu et al.2018). In Section 3 we analyze the Tycho's gamma-ray spectrum and compare it with the AMS positron flux. We find that their consistency with the theoretical predictions reaches $\chi^2/d.o.f. = 0.54$ and 0.45, respectively. This result strongly suggests that the positron excess observed by AMS mainly originates from nearby Tycho's supernova remnant. The discussions and summary are given in Section 4

2. THE GC MODEL

High energy gamma ray and electron-positron fluxes in CRs may originate from the following processes $p + p \rightarrow \pi^0 \rightarrow 2\gamma$, and $\gamma \rightarrow e^+ + e^-$. The number of secondary pions in proton-proton collision is determined by the gluon distribution inside proton (Field et al.1977). Usually, these pions have a small kinetic energy (or low momentum) at the center-of-mass (C.M.) system and form the central region in the rapidity distribution. Gluons in protons may condense at a critical momentum (x_c, k_c) . One can imagine that this GC effect should be appeared in CR spectra. A large number of gluons at the central region due to GC effects create the maximum number N_π of pions, which take up all available kinetic energy, where we neglect other secondary particles. Using general relativistic invariant and energy conservation, we have

$$(2m_p^2 + 2E_{p-p}m_p)^{1/2} = E_{p1}^* + E_{p2}^* + N_\pi m_\pi, \quad (2.1)$$

$$E_{p-p} + m_p = m_p \gamma_1 + m_p \gamma_2 + N_\pi m_\pi \gamma, \quad (2.2)$$

* Corresponding author: wzhu@phy.ecnu.edu.cn

where $E_{p_i}^*$ is the energy of leading proton at the C.M. system, γ_i are the corresponding Lorentz factors. Using the inelasticity K , we set

$$E_{p1}^* + E_{p2}^* = \left(\frac{1}{K} - 1\right)N_\pi m_\pi, \quad (2.3)$$

and

$$m_p \gamma_1 + m_p \gamma_2 = \left(\frac{1}{K} - 1\right)N_\pi m_\pi \gamma. \quad (2.4)$$

One can easily get the solutions $N_\pi(E_{p-p}, E_\pi)$ for the $p-p$ collisions

$$\ln N_\pi = 0.5 \ln E_{p-p} + a, \quad \ln N_\pi = \ln E_\pi + b, \quad (2.5)$$

$$\text{where } E_\pi \in [E_\pi^{GC}, E_\pi^{max}].$$

The parameters in the GeV unit read

$$a \equiv 0.5 \ln(2m_p) - \ln m_\pi + \ln K, \quad (2.6)$$

and

$$b \equiv \ln(2m_p) - 2 \ln m_\pi + \ln K. \quad (2.7)$$

Equation (2.5) gives the relations among N_π , E_{p-p} and E_π^{GC} by one-to-one, it leads to a following GC-characteristic spectrum.

According to the above mentioned hadronic framework of gamma-ray spectrum, we write

$$\begin{aligned} \Phi_\gamma^{GC}(E_\gamma) &= C_\gamma \left(\frac{E_\gamma}{E_\pi^{GC}}\right)^{-\beta_\gamma} \int_{E_\pi^{min}}^{E_\pi^{max}} dE_\pi \left(\frac{E_{p-p}}{E_{p-p}^{GC}}\right)^{-\beta_p} \\ &\times N_\pi(E_{p-p}, E_\pi) \frac{d\omega_{\pi-\gamma}(E_\pi, E_\gamma)}{dE_\gamma}, \end{aligned} \quad (2.8)$$

where the GC-effect enters Φ_γ^{GC} via Equation (2.5). The spectral indexes β_γ and β_p denote the propagating loss of gamma-rays and protons, respectively; C_γ incorporates the kinematic factor with the flux dimension and the percentage of $\pi^0 \rightarrow 2\gamma$. The normalized spectrum for $\pi^0 \rightarrow 2\gamma$ is

$$\frac{d\omega_{\pi-\gamma}(E_\pi, E_\gamma)}{dE_\gamma} = \frac{2}{\beta_\pi E_\pi} H\left[E_\gamma; \frac{1}{2}E_\pi(1-\beta_\pi), \frac{1}{2}E_\pi(1+\beta_\pi)\right], \quad (2.9)$$

where $H(x; a, b) = 1$ if $a \leq x \leq b$, and $H(x; a, b) = 0$ otherwise, $\beta_\pi \sim 1$. Inserting Equations (2.5)-(2.7) and (2.9) into Equation (2.8), we have

$$\begin{aligned} \Phi_\gamma^{GC}(E_\gamma) &= C_\gamma \left(\frac{E_\gamma}{E_\pi^{GC}}\right)^{-\beta_\gamma} \int_{E_\pi^{GC} \text{ or } E_\gamma}^{E_\pi^{GC, max}} dE_\pi \left(\frac{E_{p-p}}{E_{p-p}^{GC}}\right)^{-\beta_p} \\ &\times N_\pi(E_{p-p}, E_\pi) \frac{2}{\beta_\pi E_\pi}, \end{aligned} \quad (2.10)$$

where the lower-limit of the integration takes E_π^{GC} (or E_γ) if $E_\gamma \leq E_\pi^{GC}$ (or if $E_\gamma > E_\pi^{GC}$). In consequence,

$$E_\gamma^2 \Phi_\gamma^{GC}(E_\gamma) = \begin{cases} \frac{2e^b C_\gamma}{2\beta_p - 1} (E_\pi^{GC})^3 \left(\frac{E_\gamma}{E_\pi^{GC}}\right)^{-\beta_\gamma + 2} & \text{if } E_\gamma \leq E_\pi^{GC} \\ \frac{2e^b C_\gamma}{2\beta_p - 1} (E_\pi^{GC})^3 \left(\frac{E_\gamma}{E_\pi^{GC}}\right)^{-\beta_\gamma - 2\beta_p + 3} & \text{if } E_\gamma > E_\pi^{GC} \end{cases}. \quad (2.11)$$

Interestingly, this solution shows a typical broken power-law.

We add the contributions of $\gamma \rightarrow e^+ + e^-$ to Equation (2.8) and get the following positron spectrum

$$\Phi_{e^+}(E_{e^+}) = \Phi_{e^+}^0(E_{e^+}) + \Phi_{e^+}^{GC}(E_{e^+}), \quad (2.12)$$

$\Phi_{e^+}^0$ is the background flux of positron, and

$$\begin{aligned} \Phi_{e^+}^{GC}(E_{e^+}) &= C_{e^+} \left(\frac{E_{e^+}}{E_\pi^{GC}}\right)^{-\beta_{e^+}} \int_{E_{e^+}} dE_\gamma \left(\frac{E_\gamma}{E_\pi^{GC}}\right)^{-\beta_\gamma} \\ &\times \int_{E_\pi^{min}}^{E_\pi^{max}} dE_\pi \left(\frac{E_{p-p}}{E_{p-p}^{GC}}\right)^{-\beta_p} N_\pi(E_{p-p}, E_\pi) \\ &\times \frac{d\omega_{\pi-\gamma}(E_\pi, E_\gamma)}{dE_\gamma} \frac{d\omega_{\gamma-e}(E_\gamma, E_{e^+})}{dE_{e^+}} \\ &= C_{e^+} \left(\frac{E_{e^+}}{E_\pi^{GC}}\right)^{-\beta_{e^+}} \int_{E_{e^+}} \frac{dE_\gamma}{E_\gamma} \left(\frac{E_\gamma}{E_\pi^{GC}}\right)^{-\beta_\gamma} \\ &\times \int_{E_\pi^{GC} \text{ or } E_\gamma}^{E_\pi^{max}} dE_\pi \left(\frac{E_{p-p}}{E_{p-p}^{GC}}\right)^{-\beta_p} N_\pi(E_{p-p}, E_\pi) \frac{2}{\beta_\pi E_\pi} \\ &= \begin{cases} \frac{2e^b C_{e^+}}{2\beta_p - 1} E_\pi^{GC} \left(\frac{E_{e^+}}{E_\pi^{GC}}\right)^{-\beta_{e^+}} \left[\frac{1}{\beta_\gamma} \left(\frac{E_{e^+}}{E_\pi^{GC}}\right)^{-\beta_\gamma} + \left(\frac{1}{\beta_\gamma + 2\beta_p - 1} - \frac{1}{\beta_\gamma}\right) \right] & \text{if } E_{e^+} \leq E_\pi^{GC} \\ \frac{2e^b C_{e^+}}{(2\beta_p - 1)(\beta_\gamma + 2\beta_p - 1)} (E_\pi^{GC}) \left(\frac{E_{e^+}}{E_\pi^{GC}}\right)^{-\beta_{e^+} - \beta_\gamma - 2\beta_p + 1} & \text{if } E_{e^+} > E_\pi^{GC} \end{cases} \end{aligned} \quad (2.13)$$

Note that after taking average over all possible directions, the energy of pair-creation is uniformly distributed from zero to maximum value, i.e.,

$$\frac{d\omega_{\gamma-e}(E_\gamma, E_{e^+})}{dE_{e^+}} = \frac{1}{E_\gamma}. \quad (2.14)$$

Equation (2.13) shows an excess near E_π^{GC} in the positron spectrum.

3. THE EVIDENCE FOR THE GC SOURCE

The measurements of CR positron flux by AMS (Aguilar et al.2019) shows a significant excess peaked at ~ 300 GeV (or ~ 400 GeV if subtracting the contribution of the diffuse background). We try to understand it using the GC-model.

According to the GC-model Equations. (2.11) and (2.13), if the excess of positron spectrum at 400 GeV is arisen by the GC-effect, we predict: (i) one can observe gamma-ray emission originating from a same GC-source

in galaxy, which has a characteristic spectrum with a broken power-law on the two sides of $E_\gamma \simeq 400 \text{ GeV}$; (ii) the spectral indexes β_p and β_γ of this gamma-ray spectrum are same as that of the positron spectrum; (iii) the value of C_γ for this GC-source is larger than that of other similar gamma-ray sources since it is closest to the earth; (iv) this GC-source has a relatively large value of β_γ since it implies a strong $\gamma \rightarrow e^+ + e^-$ conversion mechanism.

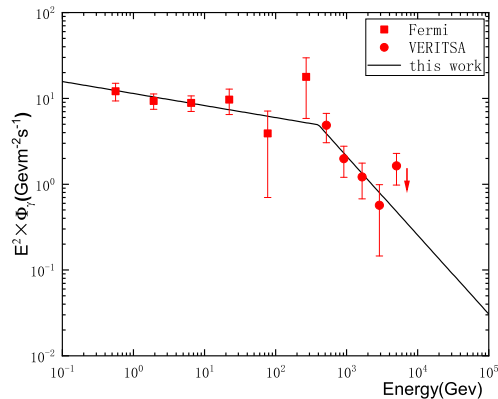


FIG. 1.— The predicted cosmic gamma-ray spectrum by the GC-model Equation (2.11) (the broken lines) and comparisons with the Fermi-LAT and VERITAS data for Tycho (Archambault et al.2017). The last point at 5 TeV is excluded since its complete uncertainty. The parameters are $E_\pi^{GC} = 400 \text{ GeV}$, $\beta_p^{Tycho} = 0.89$, $\beta_\gamma^{Tycho} = 2.14$ and $C_\gamma^{Tycho} = 6 \times 10^{-10} \text{ GeV m}^{-2} \text{ s}^{-1}$.

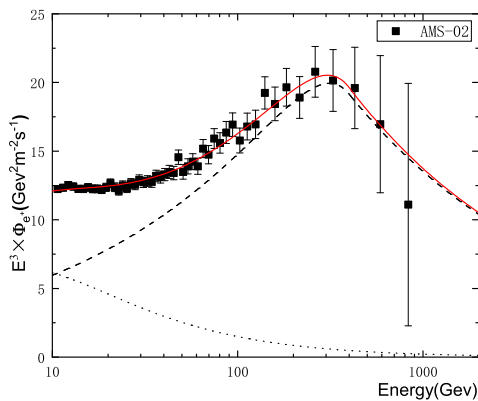


FIG. 2.— Using the GC-model Equation (2.13) (a dashed curve) to fit the positron flux (Field et al.1977). The contributions of background (a point curve) are taken from a diffuse model (Aguilar et al.2013) but the parameters are adjusted. The solid curve is a total spectrum, its $\chi^2/d.o.f. = 19.65/44$ between 10 and 10^3 GeV with the free parameters $C_{e^+} = 4.25 \times 10^{-10}$, $\beta_{e^+} = 0.460$, $\beta_\gamma^+ = 2.14$, $\beta_p^+ = 0.89$, $C_d = 0.067$, $\gamma_d = -3.86$, $E_1 = 6.33$, $E_0 = 1.13$ and $E_\pi^{GC} = 400 \text{ GeV}$.

Interestingly, supernova remnant (SNR) G120.1+1.4 is such a possible GC-source. In history it was observed

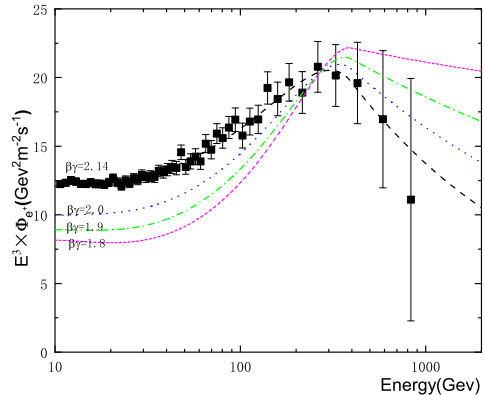


FIG. 3.— The contributions of the GC-source to the positron flux with different values of β_γ . Where the contributions of the background flux are added.

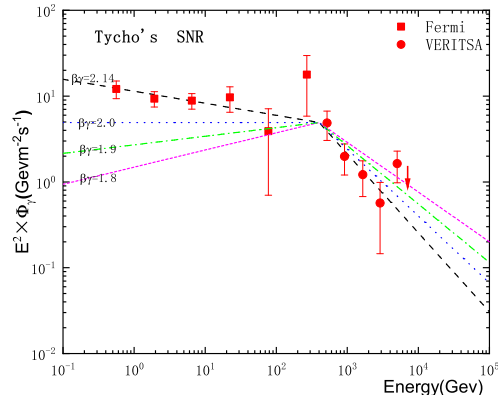


FIG. 4.— The contributions of the GC-source to the Tycho's gamma-ray flux with different values of β_γ .

by Tycho in 1572 and hereafter referred to as Tycho. An updated gamma-ray spectrum of Tycho's SNR by VERITAS and Fermi-LAT shows a clear broken power-law. Although some other models may fit the updated gamma-ray spectra after adjusting their parameters (Archambault et al.2017; Bykov et al. (2018); Cristofari et al.(2018)), as a new attempt, we try to use the GC-effect (Equation (2.11)) to fit the Tycho's spectrum. Figure 1 gives our fitting gamma-ray spectrum and the comparison with the Tycho's spectrum, where the GC-threshold $E_\pi^{GC} = 400 \text{ GeV}$, $\beta_p^{Tycho} = 0.89$, $\beta_\gamma^{Tycho} = 2.14$ and $C_\gamma^{Tycho} = 6 \times 10^{-10} \text{ GeV m}^{-2} \text{ s}^{-1}$ are fixed by the VERITAS and Fermi-LAT data. We get a reasonable fitting quality criteria

$$\chi^2/d.o.f. = \sum_i \frac{(\Phi_i^{pre} - \Phi_i^{obs})^2}{\sigma_{sys,i}^2 + \sigma_{stat,i}^2} \times \frac{1}{d.o.f.} = \frac{3.24}{6} = 0.54. \quad (3.1)$$

The one point at the high energy end of the VERITAS data is the most discrepant point relative to the fit. We noticed that the GC-threshold is nuclear mass A -dependent (see the next section). A rough estimation

shows that the GC-effect in $p-p$ collision may contribute an excess to the gamma and electron-positron spectra above 20 TeV (Zhu et al. 2018). We wait for future more sensitive measurements.

Now we assume that the excess of the positron spectrum recorded by AMS arises from Tycho's SNR. One can write the total positron flux, which is the sum of the source term Equation (2.13) and a diffuse background term (Aguilar et al.2013)

$$\Phi_{e^+}^0(E) = C_d \frac{E^2}{\hat{E}^2} \left(\frac{\hat{E}}{E_1} \right)^{\gamma_d}, \quad (3.2)$$

where $\hat{E} = E + E_0$. We substitute the fixed parameters $E_\pi^{GC} = 400 GeV$, $\beta_p^{e^+} = 0.89$ and $\beta_\gamma^{e^+} = 2.14$ into Equation (2.13) and adjust β_{e^+} , C_{e^+} and the remaining parameters in Equation (3.2). Note that $\beta_p^{e^+} = \beta_p^{Tycho}$ and $\beta_\gamma^{e^+} = \beta_\gamma^{Tycho}$ are fixed. The result is presented in Figure 2. The fitting $\chi^2/d.o.f. = 19.65/44 = 0.45$.

4. DISCUSSIONS AND SUMMARY

The conclusions of this work are based on Equations (2.1) and (2.2) under the GC-condition. This is a plausible but unproved assumption. Although the data from a range of supernova remnants including Tycho's can be approximately described by several models including leptonic and hadronic components without the GC-effect. However, the GC-effect in hadronic framework can connect two kinds of astrophysical observations perfectly, namely the positron excess in AMS and the broken power-law for Tycho's gamma ray spectrum. This feature is what we want to emphasize.

For illustrating the sensitivity of the fitting quality to the selection of the parameters, we draw the contributions of the GC-source to the positron- and gamma-ray fluxes with different values of β_γ in Figures 3 and 4, respectively. The sensitivity of the results to the parameter selection shows that our $\chi^2/d.o.f. \simeq 0.5$ is not an accidental coincidence. It seems that the high energy data points of AMS do not place significant constraints against the value of β_γ , but rather it is the low-energy Fermi-Lat points that constrain β_γ . However, considering the correlation between the low-energy point and the high-energy point, the restriction of Figures 3 and 4 on

the parameter β_γ is strict.

The results in Section 3 are consistent with our predictions: (i) $E_\pi^{GC} = 400 GeV$; (ii) $\beta_p^{Tycho} = \beta_p^{e^+}$ and $\beta_\gamma^{Tycho} = \beta_\gamma^{e^+}$.

Finally, we should explain why no GC-signals are observed at the LHC. The GC-threshold E_π^{GC} is target A -dependent, since the nonlinear term of the QCD evolution equation should be re-scaled by $A^{1/3}$ and E_π^{GC} decreases with increasing A (zhu 2017). However, A -dependence of E_π^{GC} is a complicated problem, which relates to the distribution and structure of the GC-source. We have not available input distributions of the nonlinear QCD evolution to precisely predict the GC-threshold. According to a roughly estimation in (Zhu et al. 2017), we have $E_{p-p}^{GC} > E_{p-A}^{GC} > E_{A-A}^{GC}$. Using Equations (2.1)-(2.7), the center-of-mass energy corresponding to $E_\pi^{GC} = 400 GeV$ is

$$\sqrt{S_{A-A}^{GC}} \simeq \sqrt{2m_p E_{A-A}^{GC}} = \sqrt{2m_p} e^{b-a} E_\pi^{GC} = 5.5 TeV. \quad (4.1)$$

The ALICE and ATLAS collaborations at the LHC have measured Pb-Pb (and p-Pb) collisions till $\sqrt{S_{Pb-Pb}} = 5.02 TeV$ (and $\sqrt{S_{p-Pb}} = 8.16 TeV$) (Rode et al.2019; ATLAS Collaboration 2019). We consider that $\sqrt{S_{Pb-Pb}^{GC}} > 5 TeV$ and $\sqrt{S_{p-Pb}^{GC}} > 8 TeV$, it implies that the GC-effect is entering (or will enter into) a measurable energy range.

In summary, a QCD research predicts that gluons in protons may condensed at a critical momentum in high energy collision of proton-proton. We use the GC-model to perfectly explain two seemingly completely different events of CR spectra: an excess in positron flux and the broken power-law in gamma-ray spectrum of Tycho. We consider that the excess in the CR positron spectrum observed by AMS originates mainly from the GC-effect in Tycho's supernova remnant.

ACKNOWLEDGMENTS We would like to thank the anonymous reviewer for his/her insightful comments on the manuscript. The comments have really helped us to improve our manuscript to the best possible extent. This work is supported by the National Natural Science of China (No.11851303).

REFERENCES

- Aguilar, M., et al. 2013, PhReLe, 110, 141102
Aguilar, M., et al. 2019, PhReLe, 122, 041102
Archambault, S., et al. 2017, ApJ, 836, 23
ATLAS Collaboration, 2019, arXiv: nucl-ex/1908.05264
Bykov, A.M., Ellison, D.C., Marcowith, A. et al. 2018 Space Sci Rev, 214, 41
Cristofari, P., Gabici, S., Terrier, R. and T B Humensky, T.B.,2018, Monthly Notices of the Royal Astronomical Society, 479, 3415
Feng, L., Ruan, J.H. Wang, F. & Zhu, W., 2018, ApJ, 868, 2
Field, R. D. & Feynman, R. P., 1977, PhReD, 15, 2590
Rode, S.P., et al. 2019, arXiv:hep-ex/1906.05570v2
Zhu, W., Shen, Z.Q, & Ruan, J.H., 2008, ChPhL, 25, 3605
Zhu, W., Shen, Z.Q, & Ruan, J.H., 2016, NuPhB, 911,1
Zhu, W. & Lan, J.S., 2017, NuPhB, 916, 647
Zhu, W., Lan, J.S. & Ruan, J.H, 2018, Int. J. Mod. Phys. E27,1850073